AN EXPERIMENTAL

FOUR-COMPONENT OPTICAL FIBRE BALANCE

F F Pieterse[1],
University of Johannesburg, Auckland Park, 2006, South Africa

P M Bidgood[2]
CSIR, Brummeria, Pretoria, 0001, South Africa

Conventional internal wind tunnel balances are designed to accommodate foil strain gauges, which measure the deformation (strain) of the material in the balance. Foil strain gauge balances are known to be affected by electromagnetic interference (EMI) and temperature. These balances are expensive and their manufacture is costly and time consuming. Their is always a demand for improved accuracy, higher stiffness, increased resolution and thermal stability. Alternative sensor technologies, materials, design as well as manufacturing approaches are required to reduce lead times and meet future performance requirements.

This paper outlines the design, construction and calibration of an experimental four-component internal wind tunnel balance incorporating both optical fibre and foil strain gauge sensors.

The experimental four-component balance uses the "Two-groove OFBG" (optical fibre Bragg grating) concept that was developed and demonstrated on a cantilever beam. The concept does not consider (measure) the deformation of the basic structural material (strain), but instead measures relative displacements between points in the component using optical fibres.

The "Two-groove" optical fibre concept leads to a simplified balance design with enhanced sensitivity and/or higher stiffness as well as low component interaction, thermal stability and immunity to electromagnetic interference.

Nomenclature

A	=	Area (m^2)	β	=	Wavelength-temperature sensitivity factor (pm/K)
FEM	=	Finite Element Modelling			
LSD	=	Light source diode	ΔT	=	Temperature shift (K)
n_{eff}	=	Effective index of refraction	$\Delta\varepsilon$	=	Strain
NF	=	Normal force (N)	$\Delta\lambda_{BS}$	=	Bragg wavelength Shift (nm)
P	=	Applied force (N)	Λ	=	Bragg Grating pitch (nm)
PM	=	Pitching moment (Nm)	λ	=	Bragg Wavelength (nm)
RM	=	Rolling moment (Nm)	λ_B	=	Bragg Wavelength (nm)
SF	=	Side force (N)	ν	=	Poisson's ratio
YM	=	Yawing moment (Nm)	ξ	=	Thermo-optic coefficient (/K)
α	=	Thermal expansion Coefficient of the fibre (pm/K)	ρ_α	=	Photo elastic coefficient

[1]Lecturer, Mechanical Engineering science, e-mail: ffpieterse@uj.ac.za
[2]Balance specialist, ASC (Aeronautic System Competency), e-mail: pmbidgoo@csir.co.za

I. Introduction

During the First International Symposium on Strain Gauge Balances at NASA Langley Research Centre (LaRC), Hampton, Virginia, October 1996, the symposium provided an international forum for presentation, discussion and exchange of technical information among strain-gauge balance designers[1].

One of the opening panel discussions[1] addressed the "Future Trends in Balance Development and Applications" whereby panel members, eminent balance users and designers from eight major organizations from five countries, presented their views. Some of the major requirements included, stiffer balances, balance material, temperature compensation and calibration efficiency.

At the 45th AIAA Aerospace sciences meeting and exhibit, January 2007 in Reno, Nevada, Dr Ulrich Jansen and Juergen Quest, presented a paper[2] stating:

> *"The room to move towards higher balance data quality has become very narrow and significant progress may require looking into new balance technologies, rather than just continuing to optimize existing ones".*

It is clear that designs and trends used in the last ten years do not completely fulfill all the needs expressed by the wind tunnel testing community. In the last four years the use of OFBG into wind tunnel balances was investigated and a new two groove OFBG concept was created and successfully tested on a single component balance (cantilever beam), figure 1. To evaluate this concept in a wind tunnel environment, a four-component wind tunnel balance was designed, manufacture and calibrated.

Figure 1. One component balance tested

II. The Two Groove Optical Fibre Bragg Grating (OFBG) concept

A. Optical Fibre Bragg Grating sensor (OFBG)

The Optical Fibre Bragg Grating sensor (OFBG) is one of the commercial type sensors used for strain and temperature sensing, because of its sensitivity, durability and stability. Fibre Bragg grating sensors can be manufactured with good repeatability and are becoming a popular alternative for conventional foil strain gauges.

Using a light source diode (LSD), a narrow range of the broadband wavelength of light transmitted in the fibre core is reflected back from the Bragg grating (figure 2). The reflected light is then analyzed by an optical spectrum analyzer and fed into a signal processing unit. The wavelength of light that is reflected by the Bragg grating also called the Bragg wavelength, λ_B, is determined by the grating pitch, Λ, and the effective index of refraction of the fibre core[3] , n_{eff} , (figure 2)

$$\lambda_B = 2n_{eff}\Lambda \qquad (1)$$

Up to 100 Bragg gratings can be read by an optical spectrum analyzer at any one time, provided that different Bragg wavelengths are used at each grating.

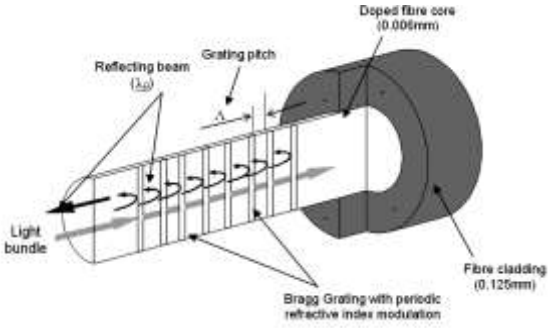

Figure 2. Reflection in an optical fibre Bragg grating

B. Strain sensing

When a force is applied to an optical fibre containing a Bragg grating, the fibre stretches causing the Bragg grating pitch, Λ, and the effective index of refraction of the fibre core, n_{eff}, to be modified. The change to the effective index of refraction of the fibre core, n_{eff}, is negligibly small compared to the increase in the Bragg grating pitch, Λ. The Bragg wavelength shift, $\Delta\lambda_{BS}$, for an applied longitudinal strain, $\Delta\varepsilon$, can be defined by the following equation[4]:

$$\Delta\lambda_{BS} = \lambda_B\left(1-\rho_\alpha\right)\Delta\varepsilon \tag{2}$$

Where ρ_α is the photo elastic coefficient of the fibre, given by

$$\rho_\alpha = \frac{n_{eff}^{\ 2}}{2}\left[\rho_{12}-\nu(\rho_{11}-\rho_{12})\right] \tag{3}$$

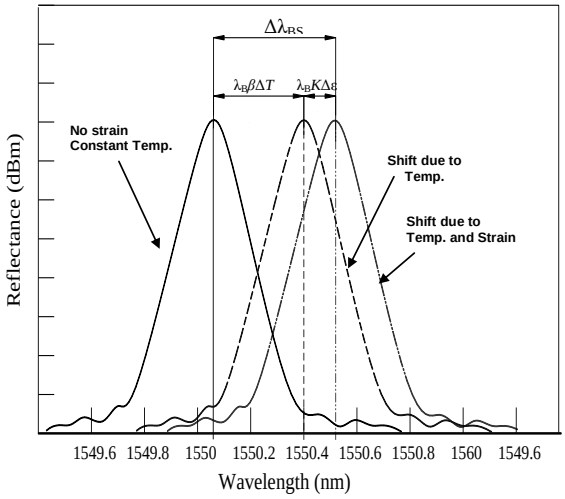

Figure 3. Wavelength shift due to strain and temperature changes

ρ_{11} and ρ_{12} are the components of the fibre strain sensor and ν the Poisson's ratio. The typical wavelength strain sensitivity for a silica fibre at 1550 nm is approx. 1.2 pm per micro strain ($\mu\varepsilon$). The Bragg wavelength shift, $\Delta\lambda_{BS}$ can be seen in figure 3.

C. Temperature sensing

It has to be noted that the Bragg wavelength shift, $\Delta\lambda_{BS}$, (figure 3), depends on the change in strain, $\Delta\varepsilon$, and the change in temperature, ΔT. The Bragg wavelength shift, $\Delta\lambda_{BS}$, can be expressed as [3]:

$$\Delta\lambda_{BS} = \lambda_B\left(1-\rho_\alpha\right)\Delta\varepsilon + \lambda_B\left(1+\xi\right)\Delta T \tag{4}$$

$$\Delta\lambda_{BS} = \lambda_B\left(K_B\Delta\varepsilon + \beta\Delta T\right) \tag{5}$$

K_B is the wavelength-strain sensitivity factor[4] ($7.8\text{x}10^{-7}/\mu\varepsilon$) and β is the wavelength-temperature sensitivity factor ($6.5\text{x}10^{-6}$/K) [4]. The wavelength change is thus much greater per degree Kelvin than that per $\mu\varepsilon$.

D. The two groove concept compensate for temperature changes and side force interactions

As shown in figure 3 the optical fibre output is influenced by both temperature and strain. The fibres on the top and the bottom groove must experience the same temperature or the temperature of each strain sensor must be measured by a second Bragg grating sensor at each fibre Bragg grating locations which is used, to compensate for any thermal interference on the measured strain.

To compensate for temperature changes and side force interactions the wavelength changes in both the grooves on the top and bottom grooves are considered, (figure 4).

Loading causes a differential change in the two OFBG sensors while a temperature change and side force interactions cause an unidirectional change in the wavelengths of the two OFBG sensors.

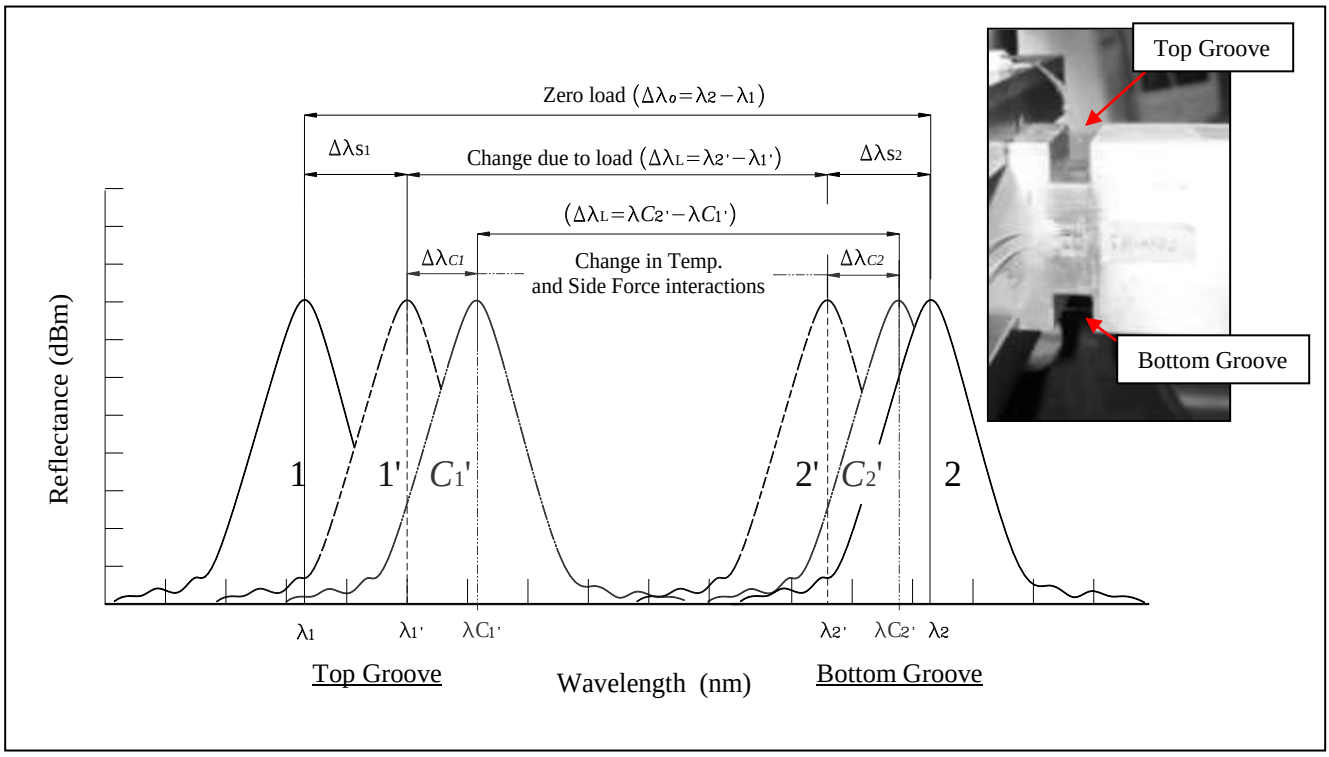

Figure 4. Wavelength affected by load, side force and temperature.

In the no-load condition, λ1 is the reflected wavelength of the fibre across the top groove and λ2 the reflected wavelength of fibre across the bottom groove. The difference between the top and bottom fibre reflected wavelengths $\Delta\lambda o = \lambda 2 - \lambda 1$. When a load is applied, the change in the reflected wavelength, Δλs1 in the top fibre is equal to the decrease in reflected wavelength, Δλs2, of the bottom fibre ($|\Delta\lambda s1| = |\Delta\lambda s2|$). The difference between the top and bottom groove fibre´s reflected wavelengths ($\Delta\lambda L = \lambda 2' - \lambda_1'$) is proportional to the displacement of the grooves relative to each other when under load and therefore proportional to the load itself.

If the two fibres (top and bottom) are at the same temperature they will have the same increase in reflected wavelength ($\Delta\lambda c_1 = \Delta\lambda c_2$). Thus the difference in reflected wavelength ($\lambda C2' - \lambda C1'$) will be equal to ($\lambda 2' - \lambda 1'$) when under load irrespective of the temperature.

For side load interactions the increase in top and bottom reflected wavelength will be equal ($\Delta\lambda c1 = \Delta\lambda c2$). The strain in both top and bottom fibres will change the same amount in the same direction as in case with temperature change. Thus, the difference in reflected wavelength ($\lambda C2' - \lambda C1'$) will be equal to ($\lambda 2' - \lambda 1'$) even in the presence of a large side force load response. This approach can be extended to the beam when in torsion or axial load. The difference ($\Delta\lambda 2' - \Delta\lambda 1'$) is therefore proportional only to bending loads applied as shown in figure 4. This is only true if both fibres do not experience different temperatures.

If the two grooves experience different temperatures ($\Delta\lambda c2 \neq \Delta\lambda c1$), an extra strain free optical fibre can be added to the top and bottom grooves to measure the temperature. The changes in reflected wavelength (Δλc1 and Δλc2) due to temperature can be deducted from the wavelengths Δλs1' and Δλs2' to compensate for their individual temperatures.

III. The design of the four-component wind tunnel balance

As for all foil strain gauge balance designs a great deal of the design is in the geometry of the balance, routing of wires and gauging the balance. As for the four-component optical fibre balance (figure 5) the following aspects were considered.

- Balance load specification
- Groove design – width, depth and spacing as well as maximum allowable fibre strain
- Optical fibre specification - Grating spacing, optical fibre Bragg grating wavelengths
- Design for manufacture
  - Gauging the balance (strain gauges) for monitoring
  - Alignment of fibres
  - Routing the fibres
  - Pre-tensioning and bonding of the fibres
- Gauging the balance (Optical fibres)
  - Location of the Bragg gratings in the fibre
  - Routing the fibres through the balance
  - Bonding and pre-tensioning of fibres across the grooves
  - Bonding of temperature fibres
- Calibration

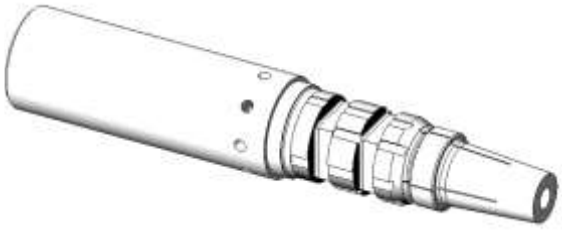

Figure 5. Four-component balance (3D sketch)

A. Design loads - Forces and moments

It was decided to use an existing calibration body used for the ø33mm balance by the CSIR[5]. By using this calibration body the four-component balance was restricted to a 33mm outside diameter and taper at the non-metric end to fit an existing sting. The balance was designed for forces and moments as specified in table 1.

Table 1. Forces and moments design criteria.

Normal Force (NF)	Pitching Moment (PM)	Side Force (SF)	Yawing Moment (YM)
2000 N	100Nm	2000 N	100Nm

B. Groove design

CosmosWorks® FEM program is used for strain calculation in the design of the four-component balance as shown in figure 6. The four-component balance design is based on the cantilever beam as shown in figure 1. The four-component balance was not designed for optimum strain gauge performance but rather to use the strain gauge bridges as a comparative reference.

Because OFBG sensors are used to measure the displacements in the grooves, the groove width and depth is limited by the Bragg grating length and strain to failure as shown in figure 7. A 5mm Bragg grating length was used. To ensure the correct positioning of the grating in the groove gap and to accommodate the selected strain gauges, a groove width of 7mm was selected.

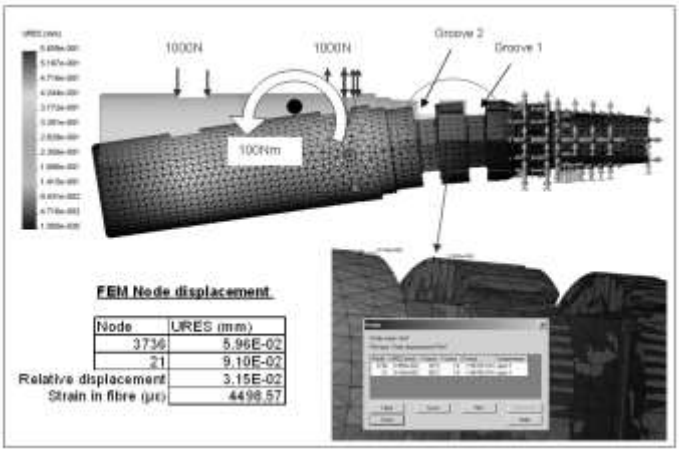

Figure 6. FEM – Strain plot

Using a FEM model the depth of the groove was determined so that the total maximum strain in the fibre would not exceed 2% (figure 7). To allow the optical fibres to measure negative displacements, the optical fibres on the top and bottom of the balance are pre-strained to 1%. Thus, under full load conditions, the top groove fibre strain will increase from 1% to 2% (1% pre-strain plus 1% strain due to load). The strain in the fibre across the bottom groove decreases from 1% to 0% (1% pre-strain minus 1% strain due to load). A 1% fibre strain (10,000με) for the chosen groove width (7mm) requires a change in groove width due to load deformation of 0.07mm. This is made a constraint in the FEM model which is then used to determine the groove depth and shape required. The same is applied to the lateral plane which is identical in load requirements.

It must be remembered that loads in one plane contribute to the strain in the fibres in the orthogonal plane (interactions) as illustrated in figure 4. The FEM model therefore has to include all combinations of loading in both planes simultaneously. Nodal displacements in the FEM model (figure 6) were used as the primary driving parameter for determining the groove depth and shape. A groove depth of 5mm (square groove) was found to give the required displacements under the applied loading conditions.

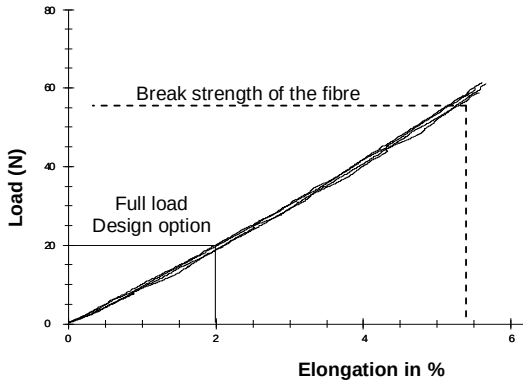

Figure 7. Fibre break test graph from FBGS Technologies [4]

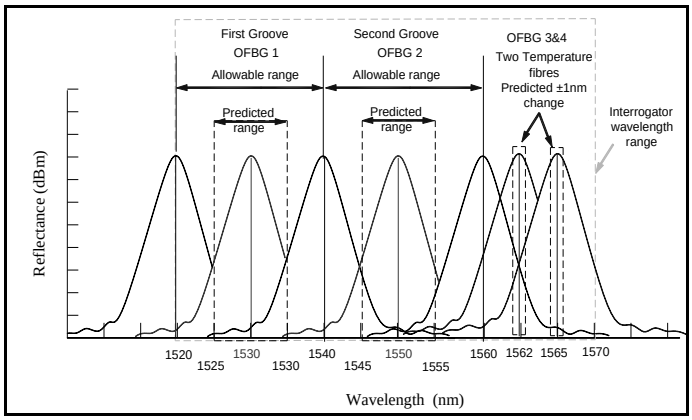

Figure 8. Optical fibre Bragg grating wavelength design

B. Groove design

It is very important to know when rolling the balance which optical fibre Bragg grating is at the top. To avoid confusion the balance is marked at 0º, 180 º and plus and minus 90 º. A groove notation was created as shown in figure 9 and used when logging the data.

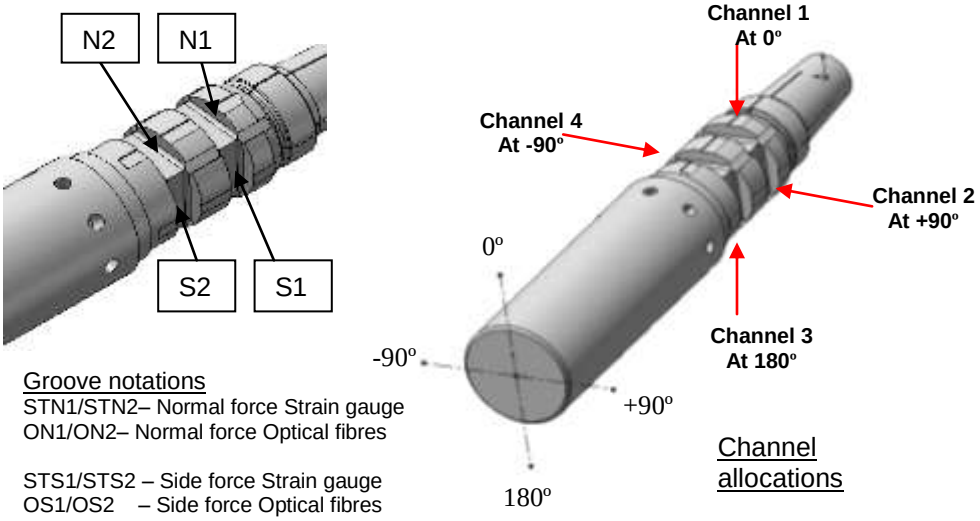

Figure 9. Calibration body orientation, groove and channel allocation

D. Manufacturing of the four-component balance

Before manufacturing the balance, a plastic model of the balance was printed using an Elite 3D printer as shown in figure 10, to evaluate the geometry of the balance and the fibre Bragg grating spacing and routing of the optical fibre. After evaluation of the plastic model, the balance was manufactured from Stainless steel 17-4 PH, heat treated to the 900H condition and ground to a ø33mm outside diameter to fit the calibration body. To overcome misalignment of the fibres across the grooves and to follow the longitudinal centre of the balance, a small 0.5mm

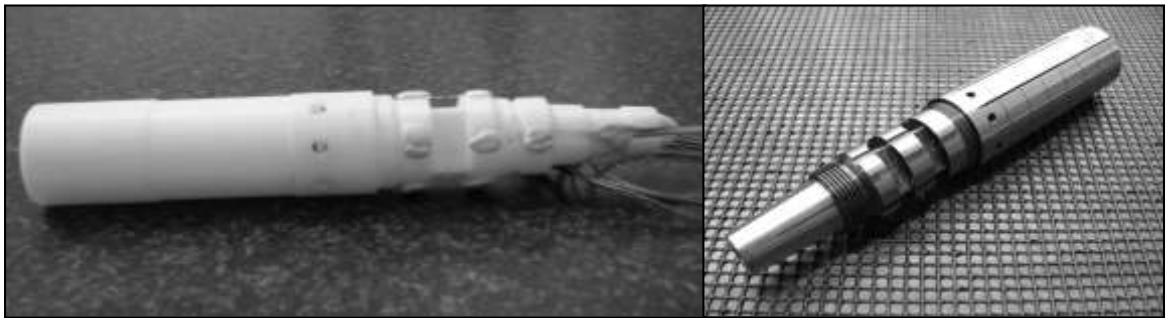

Figure 10. Plastic and stainless steel model of the balance.

cut-out is machined on the centre line of the balance. This groove facilitates accurate longitudinal alignment of the fibres across the grooves, (figure 10). If the fibres are not well aligned with respect to both the radial and longitudinal directions, orthogonal isolation of the signals will not occur. Erroneous cross-plane strains will occur in the fibres. These will be apparent as cross coupling terms in the calibration matrix and generally result in degraded uncertainty. Four thin slots were cut at the non-metric end of the balance to allow the optical fibres to protrude.

E. Strain gauges added for monitoring

This new concept using optical fibres in a balance for the first time allows for doubt and uncertainty from balance designers. To eliminate most of this uncertainty, four strain gauge bridges are added to the bottom of the grooves, as shown in figure 11, to monitor the forces and moments as a reference. Using strain gauges in the grooves gives a good understanding of the behavior of the balance independent of the quality of the calibration itself. Since the gauges are an industry accepted standard, the optical fibre data can be comparatively evaluated without issues such as load application accuracy or calibration load plan issues which may cloud performance issues. That is, the evaluation is relative rather than absolute.

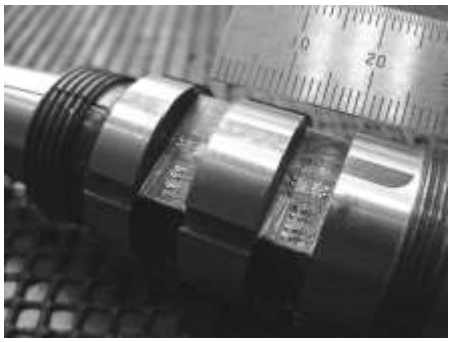

Figure 11. Strain gauges bonded in the grooves.

E. Routing of fibres

Due to the small distance between the grooves (15mm apart) and the corresponding large fibre Bragg grating spacing, (120mm apart), the fibre needed to be routed around the balance before bonding. Tensioning of the fibres in this confined space is one of the major problems to overcome. A small tensile test apparatus was modified as shown in figure 12 to accommodate the balance and fibres. Tensioning and bonding of fibres to the balance can result in breaking fibres and significant delays to the project. Therefore, trial runs with old fibres were performed to plan the method for bonding, routing, clamping and tensioning the fibres. It also provided the opportunity to get a "feel" for the fibres in this new environment. It was decided to use X60 from HBM for bonding the fibres across the grooves because of its hardness and its successful use in a commercially available bonding kit developed by Boeing and FOS&S optical

Figure 12. Optical fibre tension apparatus..

fibres. All fibres were connected to the Micron Optics four channel interrogator at all times to ensure that communication was maintained during routing, bonding and pre-tensioning of the fibres. It served as a guide to ensure that the optical fibres were pre-tensioned correctly. Care was taken when turning the balance that no fibres were hooked or bent causing failure of a fibre. The wavelengths of the Bragg gratings were monitored at all times when turning or positioning fibres. All pre-tension wavelength frequencies were captured and kept to check that no slipping of fibres occurred during balance handling, installation or calibration.

After bonding the pre-tensioned fibres across the grooves, the Bragg gratings for measuring temperature were routed and placed adjacent to the pre-tensioned Bragg grating fibres. These fibres were only bonded on one side of the grooves to allow the Bragg grating to measure temperature only as shown in figure 13.

IV. Balance calibration

A. Calibration setup

To avoid interfering with the existing equipment used for strain gauge balance calibration, it was decided to build a stand-alone system, using a NI-PCXI data acquisition system and a four channel optical fibre interrogator. The NI-PCXI data acquisition system and the four channel optical fibre interrogator were connected to a laptop computer running a Labview® program, as shown in figure 14. The HARMS calibration body was fitted to the four-component optical fibre balance, as shown in figure 15. During installation of the calibration body, all optical fibre channels were monitored for any problems that might occur.

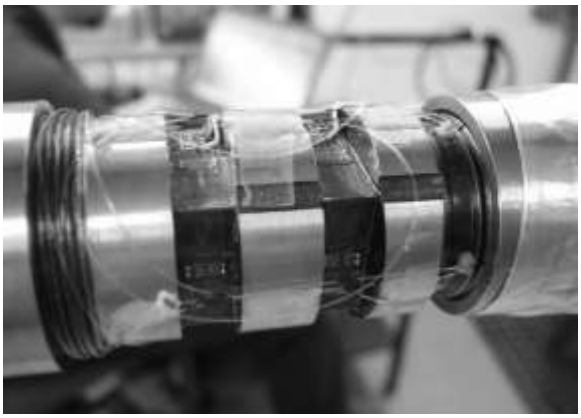

Figure 13. Optical fibre added to the balance.

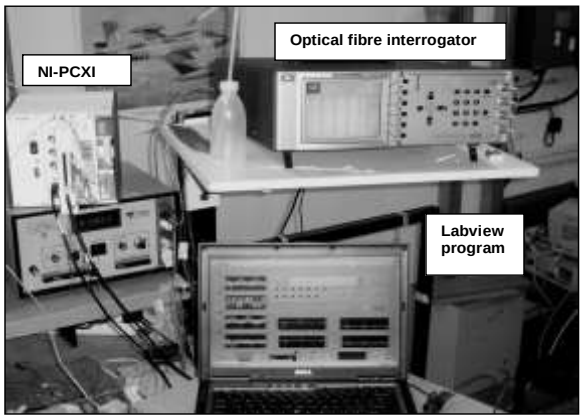

Figure 14. Optical fibre added to the balance.

Strain gauge balances have proven over the years that they are reliable, repeatable, stable and sensitive enough for most balance applications. For an optical fibre balance to be used in a wind tunnel environment, a series of tests must be conducted to prove that it is a competitive alternative for a strain gauge balance. To achieve this, an optical fibre balance was mounted on a sting and calibrated using a manual dead weight system as shown in figure 15.

B. Calibration load plan

A four-component balance has a simpler and shorter calibration load plan than a six-component balance. Because the balance is an optical fibre and strain gauge balance, the comparison of the two systems can be obtained without the use of a fully comprehensive load plan. For this reason an abbreviated load plan was used. Although the balance was designed for 2000N loads and 100Nm moments, it was decided to use normal and side forces of 1000N and pitching and yawing moment of 75Nm for the comparison.The adequacy of the two load plans was however evaluated using surface response methods prior to its use. In summary, the load plan consists of a constant force (e.g. Normal force) at seven levels, where, applied at six of these constant force levels, the pitching moment was varied between minimum and maximum. This was repeated at roll angles spaced 45º apart.

Figure 15. Calibration body fitted to the four-component optical fibre balance.

C. Sensitivity

A very small NF load set of 4.89N and high load of 1000N is used to evaluate the sensitivity and gain of the balance. The OFBG output (wavelength) from the two grooves is converted to strain (1.2 pm = 1$\mu\varepsilon$) and compared to the strain gauge output in the bottom of the grooves as mechanical gain (depth of the groove) between the two systems, (table 2). Figures 16 and 17 show the NF plots of the two systems for 4.89N and 1000N.

Table 2. Gain and sensitivity

Load	Optical fibres - ON1(με)	Strain gauges - STN1(με)	Gain
4.89N	63.98	7.74	826.61%
978.6N	2687.70	326.68	822.74%

Sensitivity	Optical fibres - ON1(με)	Strain gauges - STN1(με)
4.89N	13.08	1.58
978.6N	2.74	0.33

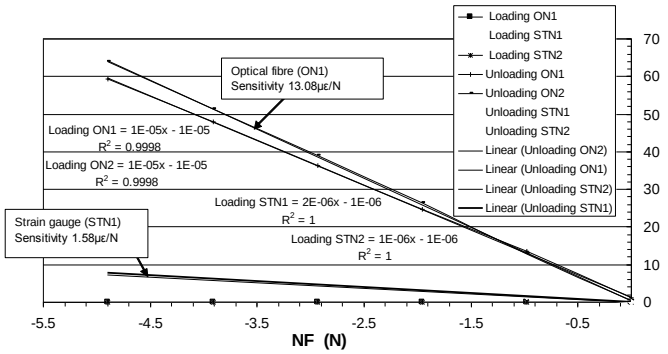

Figure 16. Sensitivity (low load).

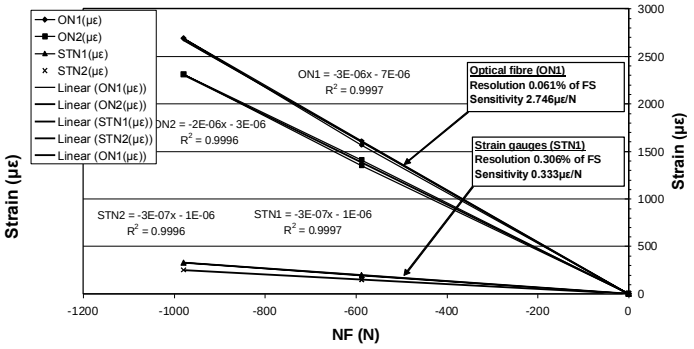

Figure 17. Sensitivity (high load).

D. Normal force and pitching moment data

The balance was loaded at 0º and 180º to a maximum NF of 1000N and a PM of 75Nm. Both the systems were logged. From the NF graphs figure 18 and 19 the similarity in the graph's can be seen. In the PM graph figure 20 (OFBG system) it can be seen that the pitching graph slope is different to the PM graph figure 21 (strain gauge system). This is due to that the first groove ON1 deformation is different to the second groove ON2. This can be compensated for in the calibration or in the design by changing the groove width.

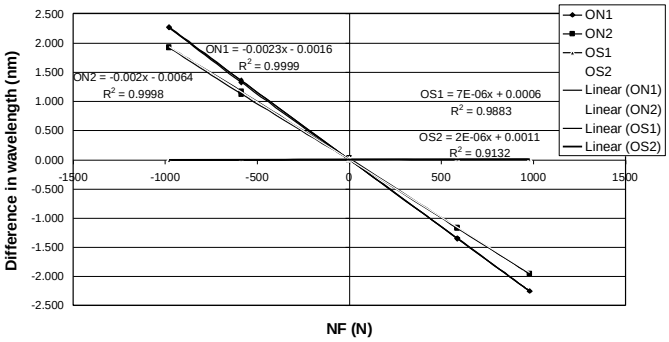

Figure 18. NF (OFBGs).

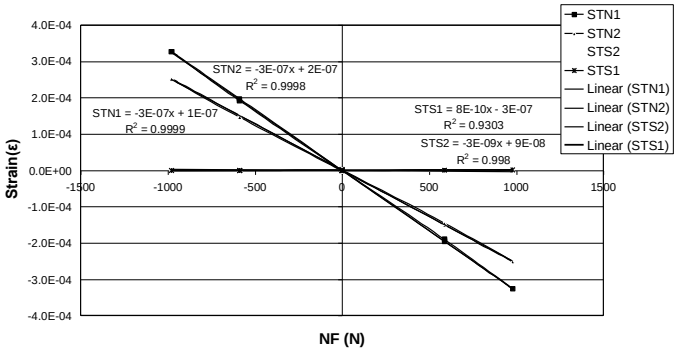

Figure 19. NF (Strain gauges).

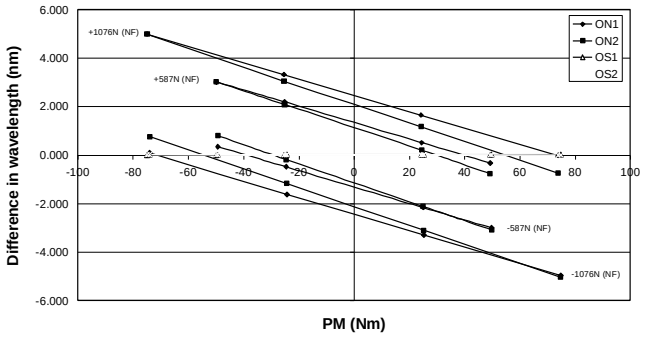

Figure 20. PM (OFBGs).

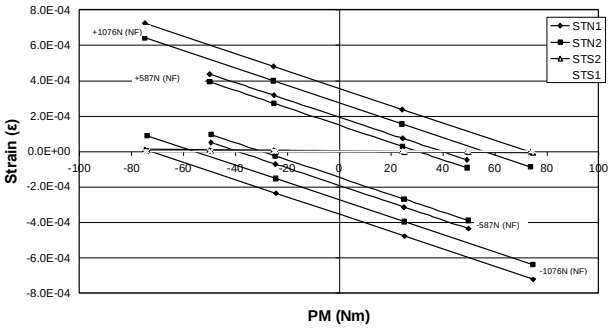

Figure 21. PM (Strain gauges).

E. Side force and yawing moment data

The balance was loaded at +90º and -90º to a maximum SF of 1000N and a YM of 75Nm. Both the systems were logged. From the SF graphs figure 22 and 23 the similarity in the graph's can be seen. In the YM graph figure 24 (OFBG system) it can again be seen that the yawing graph slope is different to the YM graph figure 25 (strain gauge system). This is due to that the first groove OS1 deformation is different to the second groove OS2. This can be compensated for in the calibration or in the design by changing the groove width.

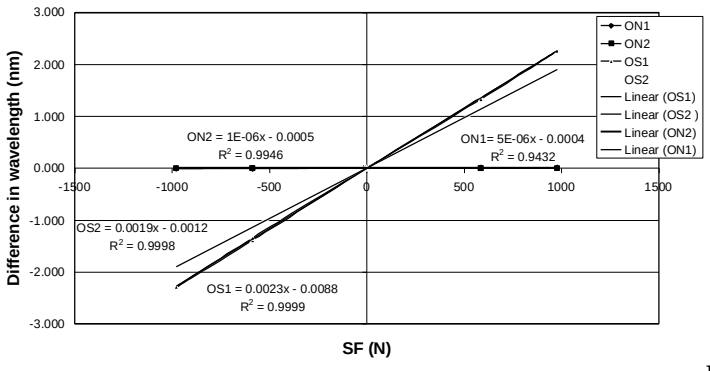

Figure 22. SF (OFBGs).

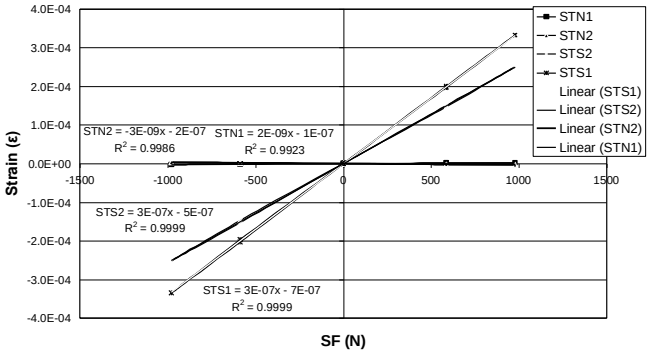

Figure 23. SF (Strain gauges).

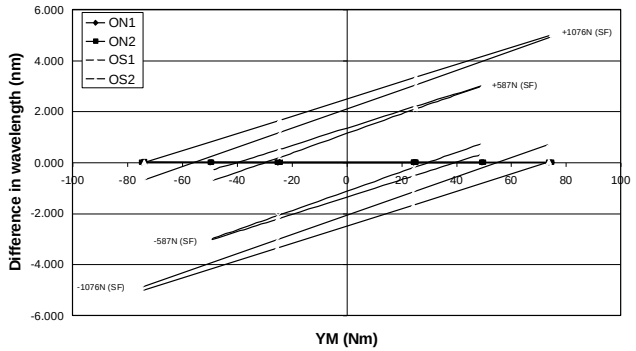

Figure 24. YM (OFBGs).

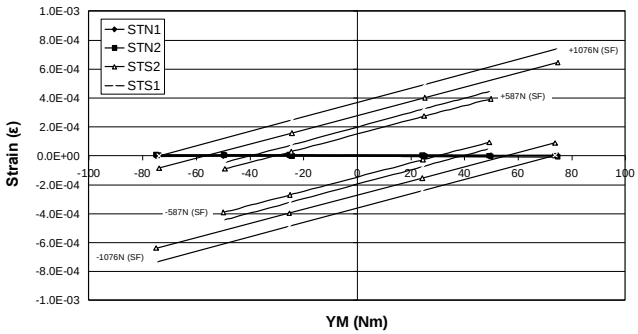

Figure 25. YM (Strain gauges).

F. Interactions

Interactions between the forces are compared as shown in table 3 and 4. It was found that the optical fibre system have less interactions as the strain gauge system.

Table 3. Intersection NF on to SF (as % of full scale).

	ON1	ON2	STN1	STN2
AVE	0.02%	0.04%	-0.01%	0.18%
Max	0.23%	0.18%	0.15%	0.97%
min	-0.19%	-0.10%	-0.25%	-0.27%
STD Deviation	0.10%	0.06%	0.10%	0.31%

Table 4. Intersection SF on to NF (as % of full scale).

	OS1	OS2	STS1	STS2
AVE	0.06%	0.02%	0.13%	0.16%
Max	0.25%	0.23%	0.56%	0.92%
min	-0.02%	-0.13%	-0.20%	-0.20%
STD Deviation	0.06%	0.07%	0.16%	0.23%

G. Thermal stability

As shown in figure 3 the strain fibres across the grooves are also affected by temperature. Because of the two grooves the thermal affect are kept to a minimum. To test this, extra fibres are fitted next to the strain fibres and bonded at one side of the groove only to measure the wavelength shift due to temperature. Calibration of the temperature fibres was done in a heat box which was placed around the balance as shown in figure 26. Thermocouples were placed around and in the calibration body to capture the temperature. The calibration showed that the strain fibres and temperature fibres experience the same wavelength shift and thus can the wavelength shift in the temperature fibres be used to compensate for temperature drift in the strain fibres.

Figure 26. Heat box

E. Reliability

The four-component optical fibre balance is as robust as the strain gauge balance supported by the fact that no optical fibre broke in gauging or in calibrating the balance. The calibration body was removed a few times and refitted to the balance. Optical fibres need to be protected to prevent damage to the fibre when routed. Optical fibres connectors need only to be plugged into an interrogator and have a minimum loss or change to the wavelength signal. For strain gauges with many connections soldered, plugged or screwed to a data acquisition system, problems such as signal loss or deterioration in voltage signal can occur. Better reliability can be expected from an optical fibre system than a wire strain gauge system.

VI. Conclusion

Replacement of strain gauge sensors with optical fibre sensors has been attempted by balance manufacturers with variable success, measuring strain of the material in the balance. Most conventional balance designs do not lend themselves to the use of optical fibres. This paper introduces an alternative approach to the use of optical fibres that does not consider the deformation of the material in a balance but instead considers the displacement of selected points in a balance measured by optical fibre strain.

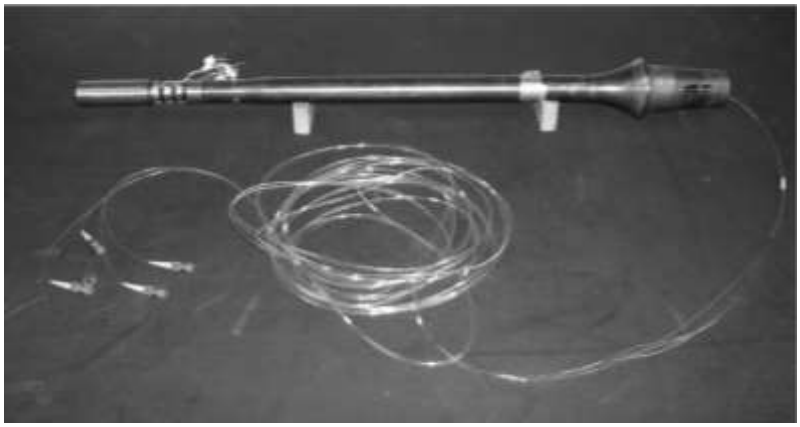

Figure 26. Four-component Optical fibre balance

The four-component balance using the Two Groove-OFBG concept can be designed, manufactured and gauged using optical fibre sensors in such a way that the four-component optical fibre balance can be successfully calibrated and a calibration matrix generated.

The Two Groove-OFBG concept used in a four component balance is a significant demonstration that it may be a competitive alternative to a strain gauge balance. This concept shows enhanced sensitivity and improved stiffness characteristics with reduced interactions and insensitivity to electromagnetic interference while also achieving increased resolution. While optical fibre Bragg gratings may be used to measure strain in any suitable environment, they may be used to great advantage in wind tunnel balances, and provide a viable alternative to foil type strain gauges.

This paper is an attempt to meet the need highlighted by Jansen and Quest in their paper[3] "SG Balance Improvements are slowing down - Europe can not wait that long".

References

[1] Summary report of the First International Symposium on Strain Gauge Balances and Workshop on AoA/Model Deformation Measurement Techniques, 1996, NASA Langley Research Centre, Hampton, Virginia, USA

[2] U Jansen and J Quest, ETW 2006, SG Balance Improvements are slowing down – Europe can not wait that long. *45th AIAA Aerospace Sciences meeting*, Volume: AIAA 207 -351, Pages 1-16

[3]YJ Rao, 1997 In-fibre Bragg grating sensors, (review article), *Measurement Science and Technology*, 8 pp.355-375.

[4]CH Chojetzi, "Data-sheet Optical Fibre Bragg Gratings", FBGS Technologies, Technologie- und Innovationspark (TIP), Jena, Germany, http://www.fbgs-technologies.com, 2008.

[5]P Bidgood, "Development of the HARMS-2b balance", *6th International Balance Symposium*, Swolle, Netherland's, May 5-8, 2008.